



Published in final edited form as:

Curr Res Neurobiol. 2021 ; 2: . doi:10.1016/j.crneur.2021.100009.

The transcriptional repressor Rev-erba regulates circadian expression of the astrocyte *Fabp7* mRNA

William M. Vanderheyden^{1,2}, Bin Fang³, Carlos C. Flores¹, Jennifer Jager⁴, Jason R. Gerstner^{1,2,5,*}

¹Elson S. Floyd College of Medicine, Washington State University, Spokane, WA. 99202, USA

²Sleep and Performance Research Center, Washington State University, Spokane, WA. 99202, USA

³Genomics Institute of the Novartis Research Foundation, 10675 John Jay Hopkins Dr, San Diego, CA 92121

⁴Université Côte d'Azur, INSERM, Centre Méditerranéen de Médecine Moléculaire (C3M), Cellular and Molecular Physiopathology of Obesity, Nice, France.

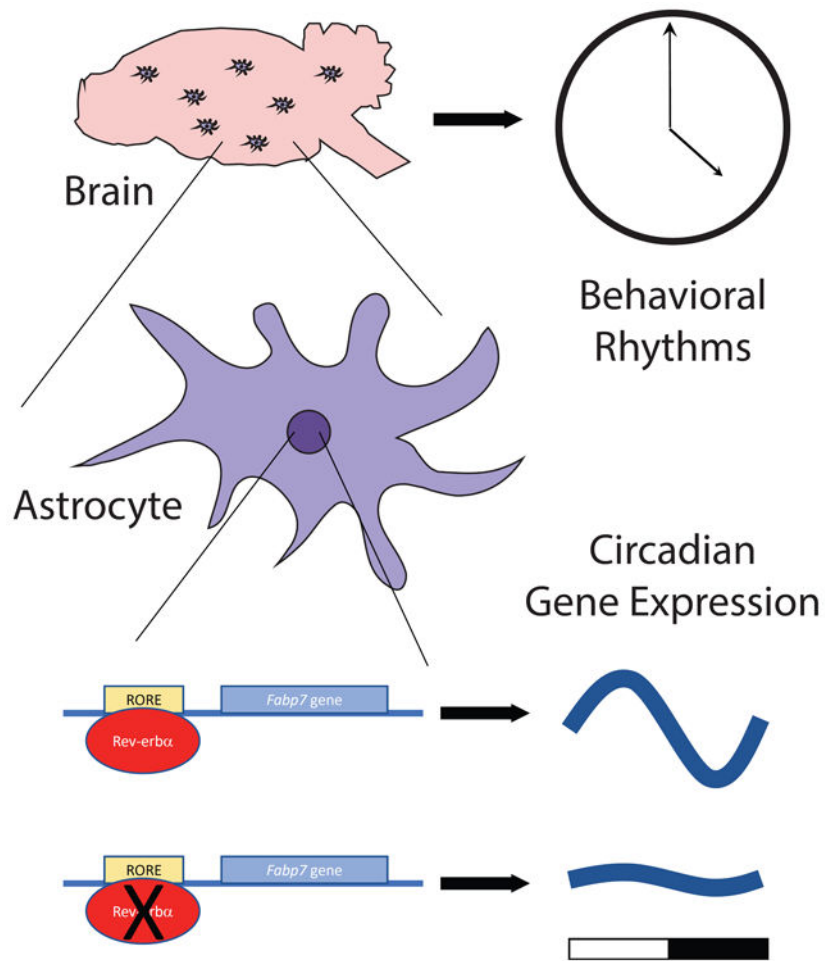
⁵Steve Gleason Institute for Neuroscience, Washington State University, Spokane, WA. 99202, USA

Abstract

The astrocyte brain-type fatty-acid binding protein (*Fabp7*) circadian gene expression is synchronized in the same temporal phase throughout mammalian brain. Cellular and molecular mechanisms that contribute to this coordinated expression are not completely understood, but likely involve the nuclear receptor Rev-erba (NR1D1), a transcriptional repressor. We performed ChIP-seq on ventral tegmental area (VTA) and identified gene targets of Rev-erba, including *Fabp7*. We confirmed that Rev-erba binds to the *Fabp7* promoter in multiple brain areas, including hippocampus, hypothalamus, and VTA, and showed that *Fabp7* gene expression is upregulated in *Rev-erba* knock-out mice. Compared to *Fabp7* mRNA levels, *Fabp3* and *Fabp5* mRNA were unaffected by *Rev-erba* depletion in hippocampus, suggesting that these effects are specific to *Fabp7*. To determine whether these effects of *Rev-erba* depletion occur broadly throughout the brain, we also evaluated *Fabp* mRNA expression levels in multiple brain areas, including cerebellum, cortex, hypothalamus, striatum, and VTA in *Rev-erba* knock-out mice. While small but significant changes in *Fabp5* mRNA expression exist in some of these areas, the magnitude of these effects are minimal to that of *Fabp7* mRNA expression, which was over 6-fold across all brain regions. These studies suggest that Rev-erba is a transcriptional repressor of *Fabp7* gene expression throughout mammalian brain.

Graphical abstract

*Corresponding author Jason R. Gerstner, j.gerstner@wsu.edu.



Keywords

lipid; metabolism; glia; BLBP; B-FABP; clock

INTRODUCTION

Fatty-acid binding proteins (Fabp) comprise a family of small (~15kDa) hydrophobic ligand binding carriers with high affinity for long-chain fatty-acids for intracellular transport, and are associated with metabolic, inflammatory, and energy homeostasis pathways (1, 2). These include three that are expressed in the adult mammalian central nervous system (CNS), and are Fabp3 (H-Fabp), Fabp5 (E-Fabp), and Fabp7 (B-Fabp). Fabp3 is primarily expressed in neurons, Fabp5 is expressed in various cell types, including both neurons and glia, and Fabp7 is most abundant in astrocytes and neural progenitors. While performing microarray analysis of transcripts in mouse brain to characterize novel diurnally regulated genes, Fabp7 was identified as a unique transcript elevated in multiple hypothalamic brain regions during the sleep phase (3). Unlike other circadian regulated gene products, Fabp7 has a synchronized pattern of global diurnal expression in adult murine brain (3-5), is regulated by the core clock gene BMAL1 (6) and has a general role in governing aspects of sleep

behavior in multiple species, including flies, mice, and humans (7). *Fabp7* has been shown to regulate dendritic morphology and excitatory cortical neuron synaptic function (8), as well as locomotor responses to NMDA-receptor activity (9), and other behavioral conditions including fear memory and anxiety (10). Therefore, *Fabp7* may play an important role in regulating time-of-day dependent changes in astrocyte-derived and evolutionarily conserved plasticity-related processes (11-13).

Here we were interested in validating findings that *Fabp7* is a target of Rev-erba (14) and determining whether *Fabp7* mRNA is regulated by Rev-erba across multiple brain areas. We also wanted to examine whether these effects are specific to *Fabp7*, or whether other *Fabps* expressed in the CNS are similarly affected.

RESULTS

Since the time-of-day profile of *Fabp7* mRNA expression is abolished in BMAL1 KO mice (6), we performed bioinformatic analysis to locate core canonical E-box elements (CACGTG) within the *Fabp7* promoter. We did not detect any canonical E-box elements, so we considered whether other cis-acting elements influenced by circadian output in the *Fabp7* promoter exist. Analysis of the promoter for *Fabp7* gene revealed several sites known to be involved in the metabolic arm of the clock (15-17), including multiple sites for the transcriptional co-repressor nuclear receptor Rev-erba (NR1D1), termed Rev-erba response elements (RORE) (TABLE S1).

To determine whether these RORE sites were functional, we performed chromatin immunoprecipitation experiments followed by DNA-sequencing (ChIP-seq) on tissue from the ventral tegmental area (VTA), a brain region known to regulate motivational/reward behaviors (18, 19), wakefulness, and sleep (20-22). Here we identified positive Rev-erba interactions within the first kilobase upstream of the transcription start site of the *Fabp7* promoter, but not in the *Fabp3* or *Fabp5* promoters (Figure 1A-C). The top 20 Rev-erba binding site loci, peak score, distance to the translational start site and gene names are listed in Table 1. Gene Ontology (GO) analysis revealed significant enrichment of several biological processes, molecular functions, and cellular components (Table 2) and Kyoto Encyclopedia of Genes and Genomes (KEGG) analysis shows the top 20 pathways in Rev-erba ChIP-seq genes (Figure 2). The complete list of Rev-erba ChIP-seq genes is provided in [SUPPLEMENTAL dataset 1].

To confirm that Rev-erba binds the *Fabp7* promoter in multiple brain regions, we compared Rev-erba binding in the *Fabp7* promoter against the negative control *insulin*, and the positive control *NPAS2* in WT and Rev-erba KO mice. We observed Rev-erba binding to the *Fabp7* and *NPAS2* promoters in WT, but not Rev-erba KO mice, in both hippocampus (Figure 3A) and hypothalamus (Figure 3B). Binding of Rev-erba was not observed for *insulin*, regardless of genotype (Figure 3A, B). Since BMAL1 is known to transactivate Rev-erba (23, 24), a transcriptional repressor, BMAL1 could influence *Fabp7* gene expression (6) indirectly through Rev-erba.

To test the hypothesis that Rev-erba represses *Fabp7* gene expression, we examined the diurnal profile of *Fabp7* mRNA in Rev-erba KO mice. If *Fabp7* expression is repressed by Rev-erba, this predicts that *Fabp7* mRNA should be elevated in the Rev-erba KO. We confirmed that *Fabp7* mRNA is elevated in hippocampus of Rev-erba KO mice, while *Fabp3* and *Fabp5* mRNA levels are not affected (Figure 4A-C). To determine whether time-of-day mRNA levels are affected by Rev-erba, we analyzed the normalized mRNA expression for *Fabp3*, *Fabp5*, and *Fabp7* from six time-points over 24h of Rev-erba KO and WT mice. While *Fabp3* (Figure 4D) and *Fabp5* (Figure 4E) mRNA do not oscillate in WT mice and remain unaffected in Rev-erba KOs, the *Fabp7* mRNA circadian oscillation is disrupted in the Rev-erba KO compared to WT hippocampus (Figure 4F). Since *Fabp7* expression is diurnally regulated throughout murine brain (3-5), we wanted to determine if *Fabp7* mRNA levels were regulated by Rev-erba broadly in multiple brain regions. Analysis of multiple brain regions including striatum, VTA, cerebellum, hippocampus, hypothalamus, and cortex of Rev-erba KO compared to WT mice revealed analogous increases in *Fabp7* mRNA levels (~6-15 fold), but not *Fabp3* or *Fabp5* mRNA levels (Figure 5). Together, these data suggest that the circadian clock control of *Fabp7* mRNA expression requires Rev-erba broadly across many brain regions.

DISCUSSION

The astrocyte *Fabp7* gene expression is known to cycle in a synchronized fashion throughout the mammalian CNS (3-5, 14). Previous studies have shown *Fabp7* circadian gene expression is under control of the core clock transcription factor BMAL1 (6), however the *Fabp7* promoter lacks a canonical E-box element, suggesting that BMAL1 may indirectly exert its effects on *Fabp7* circadian expression via Rev-erba, a transcriptional repressor, and known BMAL1 target (25). Here we provide evidence that *Fabp7* contains canonical ROREs and that Rev-erba binds to the RORE regions in the *Fabp7* gene locus in the VTA (Figure 1A). The current study validates a previous report that also showed Rev-erba binding to *Fabp7* in the hippocampus (14) (Figure 3A), and extends these findings to show this also occurs in the hypothalamus (Figure 3B). Taken together, these results suggest that the coordinated and synchronized expression of *Fabp7* transcription is controlled by Rev-erba direct binding in multiple brain regions throughout mammalian brain.

Rev-erba KO mice showed a greater than 6-fold increase in *Fabp7* mRNA expression across multiple brain areas, including cerebellum, cortex, hippocampus, hypothalamus, striatum, and VTA, compared to WT mice. We also observed minimal, but significant, reduction in *Fabp5* mRNA in a few brain areas (cerebellum, hypothalamus, and VTA; Figure 5) and no differences in *Fabp3* mRNA in any brain region, in Rev-erba KO compared to WT mice. These reductions in *Fabp5* mRNA may represent compensatory mechanisms that are in response to the large increases in *Fabp7* mRNA expression in glial cells, however, to rule out a direct role of Rev-erba in transcriptional regulation of these other *Fabp* types throughout brain, binding assays for Rev-erba at their respective genetic loci across multiple brain regions would be required. Recently, local oscillators have been discovered in multiple brain regions throughout the mammalian brain (26), therefore it will be important to determine the extent to which *Fabp7* oscillations require ‘global’ vs. ‘local’ coordinated control. Stability of Rev-erba and the role of degradation processes that control the protein half-life in

downstream signaling may also contribute to alterations in periodicity of gene expression (27). Future studies determining the cell-type specificity of these observations are also needed to better understand lipid-mediated signaling cascades (28, 29) downstream of circadian- and metabolically (16, 30-32) driven changes in *Rev-erba* expression both within and between neurons and glia.

Understanding the molecular and cellular components that regulate *Fabp7* expression will have important implications for public health. For example, pathological states associated with *Fabp7* overexpression exist for a variety of diseases, including multiple types of cancer (33-38), and neurodegenerative disease, including Alzheimer's disease (39, 40). Given the role of the circadian clock in cancer (41-43) and neurodegeneration (44-46), future studies determining the role in how circadian *Fabp7* and *Fabp7* lipid-signaling may feedback onto metabolic (15, 31, 47) and inflammatory pathways (48-50) may provide novel links between clock-regulated mechanisms, fatty-acid pathways, and disease.

MATERIALS AND METHODS

Animals.

The *Rev-erba* knock out (KO) mice were obtained from B. Vennström and were backcrossed for >7 generations with C57/B16 mice. Mice (N=3-7 per group) were housed under standard 12h-light/12h-dark (LD) cycles and were sacrificed at specific times (zeitgeber time (ZT) 2, 6, 10, 14, 18, 22 with ZT0 corresponding to 7 a.m.). Animal care and use procedures followed the guidelines of the Institutional Animal Care and Use Committee of the University of Pennsylvania in accordance with the guidelines of the US National Institutes of Health.

Chromatin immunoprecipitation (ChIP).

ChIP experiments were performed as previously described (51) with minor changes. Mouse brain tissue was harvested at ZT10, minced and cross-linked in 1% formaldehyde for 20min, followed by quenching with 1/20 volume of 2.5M glycine solution for 5 minutes, and then two washes with PBS. Cell lysates with fragmented chromatin were prepared by probe sonication in ChIP dilution buffer (50mM HEPES, 155mM NaCl, 1.1% Triton X-100, 0.11% sodium deoxycholate, 0.1% SDS, 1mM phenylmethylsulfonyl fluoride [PMSF], and a complete protease inhibitor tablet [pH 7.5]). Proteins were immunoprecipitated in ChIP dilution buffer, using 1 µg of *Rev-erba* antibody (Cell signaling). Cross-linking was reversed overnight at 65°C in elution buffer (50mM Tris-HCL, 10mM EDTA, 1% SDS, pH8), and DNA isolated using phenol/chloroform/isoamyl alcohol. Precipitated DNA was analyzed by quantitative PCR or high-throughput sequencing.

ChIP-qPCR.

Precipitated DNA was analyzed by quantitative PCR, using the following primers: *Fabp7*, forward: 5'-GGG GAT CAG GAT TGT GAT GT-3'; *Fabp7*, reverse: 5'-AGA TGG CTC CAA TCC TCC TT-3'; *Arbp*, forward: 5'- CTG GGA CGA TGA ATG AGG AT-3'; *Arbp*, reverse: 5'- AGC AGC TGG CAC CTA AAC AG-3'; *Npas2*, forward: 5'-TTG CAG AAG CTT GGG AAA AG-3'; *Npas2*, reverse: 5'-TTT CCT GTG GGA GGA GAC AG-3'.

ChIP-seq and cistromic analysis.

For ChIP-seq, material from three mice was pooled prior to library generation. ChIP DNA was prepared for sequencing according to the amplification protocol provided by Illumina, using adaptor oligo and primers from Illumina, enzymes from New England Biolabs and PCR Purification Kit and MinElute Kit from Qiagen. Deep sequencing was performed by the Functional Genomics Core (J. Schug and K. Kaestner) of the Penn Diabetes Endocrinology Research Center using the Illumina HiSeq2000, and sequences were obtained using the Solexa Analysis Pipeline. Sequenced reads were aligned to the mouse reference genome (mm9) and peak calling was performed with HOMER (52). ChIP-seq data are deposited in NCBI GEO GSE67973 (17), for GSM1659684 and GSM1659685 datasets.

MEME Package—Analysis of the Fabp7 promoter was done using the MEME package (<http://meme.nbcr.net/meme/>). 2000 base pairs upstream and 2000 base pairs downstream of the murine Fabp7 transcription start site (TSS) was used for promoter analysis. Reference to site location of cis-elements were expressed 0-4000, with 2000 being at the TSS.

GO and KEGG Analysis—Gene ontology analysis was performed on the ranked list of Rev-erba ChIP-seq genes with peak score >2 [SUPPLEMENTAL dataset 1], using Panther GO-Slim against the mouse gene list (<http://geneontology.org> release 2021-01-01: 44,091; (53, 54). Top non-redundant categories are presented.

KEGG pathway analysis was performed on the same gene list using KEGG Mapper https://www.genome.jp/kegg/tool/map_pathway1.html (55) against mouse pathways.

qPCR—Total RNA was extracted from tissue using the RNeasy Mini Kit (QIAGEN) and treated with DNase (QIAGEN). The RNA was reversed transcribed using the High-Capacity cDNA Reverse Transcription kit (Applied Biosystems) and analyzed by quantitative PCR. Quantitative PCR was performed with Power SYBR Green PCR Mastermix on the PRISM 7500 (Applied Biosystems). Gene expression was normalized to mRNA levels of housekeeping gene 36B4 and the level of the gene of interest in the control samples. Circadian oscillations in gene expression were calculated using JTK_cyclev3.1 scripts (56) run on R. Amplitude confidence intervals were calculated according to Miyazaki et al., 2011 (57).

Primers: 36B4 Forward TCC-AGG-CTT-TGG-GCA-TCA-3';

36B4 Reverse CTT-TAT-CAG-CTG-CAC-ATC-ACT-CAG-A

Fabp3 Forward CTG-ACT-CTC-ACT-CAT-GGC-AGT-GT

Fabp3 Reverse GCC-AGG-TCA-CGC-CTC-CTT

Fabp5 Forward CGA-CAG-CTG-ATG-GCA-GAA-AAA

Fabp5 Reverse GAC-CAG-GGC-ACC-GTC-TTG

Fabp7 Forward CTC-TGG-GCG-TGG-GCT-TT

Fabp7 Reverse TTC-CTG-ACT-GAT-AAT-CAC-AGT-TGG-TT

Supplementary Material

Refer to Web version on PubMed Central for supplementary material.

Acknowledgements:

We would like to thank Dr. A. Pack and the UPENN Center for Sleep and Circadian Neurobiology and Dr. M. Lazar and the UPENN Institute for Diabetes, Obesity, and Metabolism for advice and support.

Funding:

This work was supported by National Institute of Health grant R35GM133440 to J.R.G.

REFERENCES

1. Furuhashi M, Hotamisligil GS, Fatty acid-binding proteins: role in metabolic diseases and potential as drug targets. *Nat Rev Drug Discov* 7, 489–503 (2008). [PubMed: 18511927]
2. Storch J, Corsico B, The emerging functions and mechanisms of mammalian fatty acid-binding proteins. *Annu Rev Nutr* 28, 73–95 (2008). [PubMed: 18435590]
3. Gerstner JR, Vander Heyden WM, Lavaute TM, Landry CF, Profiles of novel diurnally regulated genes in mouse hypothalamus: expression analysis of the cysteine and histidine-rich domain-containing, zinc-binding protein 1, the fatty acid-binding protein 7 and the GTPase, ras-like family member 11b. *Neuroscience* 139, 1435–1448 (2006). [PubMed: 16517089]
4. Gerstner JR et al., Brain fatty acid binding protein (Fabp7) is diurnally regulated in astrocytes and hippocampal granule cell precursors in adult rodent brain. *PLoS One* 3, e1631 (2008). [PubMed: 18286188]
5. Gerstner JR et al., Time of day regulates subcellular trafficking, tripartite synaptic localization, and polyadenylation of the astrocytic Fabp7 mRNA. *J Neurosci* 32, 1383–1394 (2012). [PubMed: 22279223]
6. Gerstner JR, Paschos GK, Circadian expression of Fabp7 mRNA is disrupted in Bmal1 KO mice. *Mol Brain* 13, 26 (2020). [PubMed: 32093736]
7. Gerstner JR et al., Normal sleep requires the astrocyte brain-type fatty acid binding protein FABP7. *Sci Adv* 3, e1602663 (2017). [PubMed: 28435883]
8. Ebrahimi M et al., Astrocyte-expressed FABP7 regulates dendritic morphology and excitatory synaptic function of cortical neurons. *Glia* 64, 48–62 (2016). [PubMed: 26296243]
9. Watanabe A et al., Fabp7 maps to a quantitative trait locus for a schizophrenia endophenotype. *PLoS Biol* 5, e297 (2007). [PubMed: 18001149]
10. Owada Y et al., Altered emotional behavioral responses in mice lacking brain-type fatty acid-binding protein gene. *Eur J Neurosci* 24, 175–187 (2006). [PubMed: 16882015]
11. Lavialle M et al., Structural plasticity of perisynaptic astrocyte processes involves ezrin and metabotropic glutamate receptors. *Proc Natl Acad Sci U S A* 108, 12915–12919 (2011). [PubMed: 21753079]
12. Nagai J et al., Behaviorally consequential astrocytic regulation of neural circuits. *Neuron*, (2020).
13. Gerstner JR, On the evolution of memory: a time for clocks. *Front Mol Neurosci* 5, 23 (2012). [PubMed: 22403527]
14. Schnell A et al., The nuclear receptor REV-ERB α regulates Fabp7 and modulates adult hippocampal neurogenesis. *PLoS One* 9, e99883 (2014). [PubMed: 24932636]
15. Cho H et al., Regulation of circadian behaviour and metabolism by REV-ERB- α and REV-ERB- β . *Nature* 485, 123–127 (2012). [PubMed: 22460952]
16. Bugge A et al., Rev-erbalpha and Rev-erbbeta coordinately protect the circadian clock and normal metabolic function. *Genes Dev* 26, 657–667 (2012). [PubMed: 22474260]

17. Zhang Y et al., GENE REGULATION. Discrete functions of nuclear receptor Rev-erba couple metabolism to the clock. *Science* 348, 1488–1492 (2015). [PubMed: 26044300]
18. Morales M, Margolis EB, Ventral tegmental area: cellular heterogeneity, connectivity and behaviour. *Nat Rev Neurosci* 18, 73–85 (2017). [PubMed: 28053327]
19. Russo SJ, Nestler EJ, The brain reward circuitry in mood disorders. *Nat Rev Neurosci* 14, 609–625 (2013). [PubMed: 23942470]
20. Takata Y et al., Sleep and Wakefulness Are Controlled by Ventral Medial Midbrain/Pons GABAergic Neurons in Mice. *J Neurosci* 38, 10080–10092 (2018). [PubMed: 30282729]
21. Yu X et al., GABA and glutamate neurons in the VTA regulate sleep and wakefulness. *Nat Neurosci* 22, 106–119 (2019). [PubMed: 30559475]
22. Eban-Rothschild A, Rothschild G, Giardino WJ, Jones JR, de Lecea L, VTA dopaminergic neurons regulate ethologically relevant sleep-wake behaviors. *Nat Neurosci* 19, 1356–1366 (2016). [PubMed: 27595385]
23. Mohawk JA, Green CB, Takahashi JS, Central and peripheral circadian clocks in mammals. *Annu Rev Neurosci* 35, 445–462 (2012). [PubMed: 22483041]
24. Albrecht U, Timing to perfection: the biology of central and peripheral circadian clocks. *Neuron* 74, 246–260 (2012). [PubMed: 22542179]
25. Guillaumond F, Dardente H, Giguère V, Cermakian N, Differential control of Bmal1 circadian transcription by REV-ERB and ROR nuclear receptors. *J Biol Rhythms* 20, 391–403 (2005). [PubMed: 16267379]
26. Paul JR et al., Circadian regulation of membrane physiology in neural oscillators throughout the brain. *Eur J Neurosci*, (2019).
27. DeBruyne JP, Baggs JE, Sato TK, Hogenesch JB, Ubiquitin ligase Siah2 regulates RevErba degradation and the mammalian circadian clock. *Proc Natl Acad Sci U S A* 112, 12420–12425 (2015). [PubMed: 26392558]
28. Gooley JJ, Chua EC, Diurnal regulation of lipid metabolism and applications of circadian lipidomics. *J Genet Genomics* 41, 231–250 (2014). [PubMed: 24894351]
29. Gooley JJ, Circadian regulation of lipid metabolism. *Proc Nutr Soc* 75, 440–450 (2016). [PubMed: 27225642]
30. Kumar Jha P, Challet E, Kalsbeek A, Circadian rhythms in glucose and lipid metabolism in nocturnal and diurnal mammals. *Mol Cell Endocrinol* 418 Pt 1, 74–88 (2015). [PubMed: 25662277]
31. Bass J, Takahashi JS, Circadian integration of metabolism and energetics. *Science* 330, 1349–1354 (2010). [PubMed: 21127246]
32. Eckel-Mahan K, Sassone-Corsi P, Metabolism and the circadian clock converge. *Physiol Rev* 93, 107–135 (2013). [PubMed: 23303907]
33. Zhou J et al., Overexpression of FABP7 promotes cell growth and predicts poor prognosis of clear cell renal cell carcinoma. *Urol Oncol* 33, 113.e119–117 (2015).
34. Liu RZ et al., A fatty acid-binding protein 7/RXRβ pathway enhances survival and proliferation in triple-negative breast cancer. *J Pathol* 228, 310–321 (2012). [PubMed: 22322885]
35. Mita R, Beaulieu MJ, Field C, Godbout R, Brain fatty acid-binding protein and omega-3/omega-6 fatty acids: mechanistic insight into malignant glioma cell migration. *J Biol Chem* 285, 37005–37015 (2010). [PubMed: 20834042]
36. Cordero A et al., FABP7 is a key metabolic regulator in HER2+ breast cancer brain metastasis. *Oncogene* 38, 6445–6460 (2019). [PubMed: 31324889]
37. Kagawa Y et al., Role of FABP7 in tumor cell signaling. *Adv Biol Regul* 71, 206–218 (2019). [PubMed: 30245263]
38. Ma R et al., FABP7 promotes cell proliferation and survival in colon cancer through MEK/ERK signaling pathway. *Biomed Pharmacother* 108, 119–129 (2018). [PubMed: 30218856]
39. Teunissen CE et al., Brain-specific fatty acid-binding protein is elevated in serum of patients with dementia-related diseases. *Eur J Neurol* 18, 865–871 (2011). [PubMed: 21143341]

40. Johnson ECB et al., Deep proteomic network analysis of Alzheimer's disease brain reveals alterations in RNA binding proteins and RNA splicing associated with disease. *Mol Neurodegener* 13, 52 (2018). [PubMed: 30286791]
41. Masri S, Sassone-Corsi P, The emerging link between cancer, metabolism, and circadian rhythms. *Nat Med* 24, 1795–1803 (2018). [PubMed: 30523327]
42. Sulli G, Lam MTY, Panda S, Interplay between Circadian Clock and Cancer: New Frontiers for Cancer Treatment. *Trends Cancer* 5, 475–494 (2019). [PubMed: 31421905]
43. Sulli G, Manoogian ENC, Taub PR, Panda S, Training the Circadian Clock, Clocking the Drugs, and Drugging the Clock to Prevent, Manage, and Treat Chronic Diseases. *Trends Pharmacol Sci* 39, 812–827 (2018). [PubMed: 30060890]
44. Musiek ES, Holtzman DM, Mechanisms linking circadian clocks, sleep, and neurodegeneration. *Science* 354, 1004–1008 (2016). [PubMed: 27885006]
45. Hood S, Amir S, Neurodegeneration and the Circadian Clock. *Front Aging Neurosci* 9, 170 (2017). [PubMed: 28611660]
46. Lananna BV et al., Chi311/YKL-40 is controlled by the astrocyte circadian clock and regulates neuroinflammation and Alzheimer's disease pathogenesis. *Sci Transl Med* 12, (2020).
47. Panda S, Circadian physiology of metabolism. *Science* 354, 1008–1015 (2016). [PubMed: 27885007]
48. Carter SJ et al., A matter of time: study of circadian clocks and their role in inflammation. *J Leukoc Biol* 99, 549–560 (2016). [PubMed: 26856993]
49. Scheiermann C, Kunisaki Y, Frenette PS, Circadian control of the immune system. *Nat Rev Immunol* 13, 190–198 (2013). [PubMed: 23391992]
50. Castanon-Cervantes O et al., Dysregulation of inflammatory responses by chronic circadian disruption. *J Immunol* 185, 5796–5805 (2010). [PubMed: 20944004]
51. Feng D et al., A circadian rhythm orchestrated by histone deacetylase 3 controls hepatic lipid metabolism. *Science* 331, 1315–1319 (2011). [PubMed: 21393543]
52. Heinz S et al., Simple combinations of lineage-determining transcription factors prime cis-regulatory elements required for macrophage and B cell identities. *Mol Cell* 38, 576–589 (2010). [PubMed: 20513432]
53. Ashburner M et al., Gene ontology: tool for the unification of biology. The Gene Ontology Consortium. *Nat Genet* 25, 25–29 (2000).
54. The Gene Ontology resource: enriching a GOld mine. *Nucleic Acids Res* 49, D325–d334 (2021). [PubMed: 33290552]
55. Kanehisa M, Sato Y, KEGG Mapper for inferring cellular functions from protein sequences. *Protein Sci* 29, 28–35 (2020). [PubMed: 31423653]
56. Hughes ME, Hogenesch JB, Kornacker K, JTK_CYCLE: an efficient nonparametric algorithm for detecting rhythmic components in genome-scale data sets. *J Biol Rhythms* 25, 372–380 (2010). [PubMed: 20876817]
57. Miyazaki M et al., Age-associated disruption of molecular clock expression in skeletal muscle of the spontaneously hypertensive rat. *PLoS One* 6, e27168 (2011). [PubMed: 22076133]

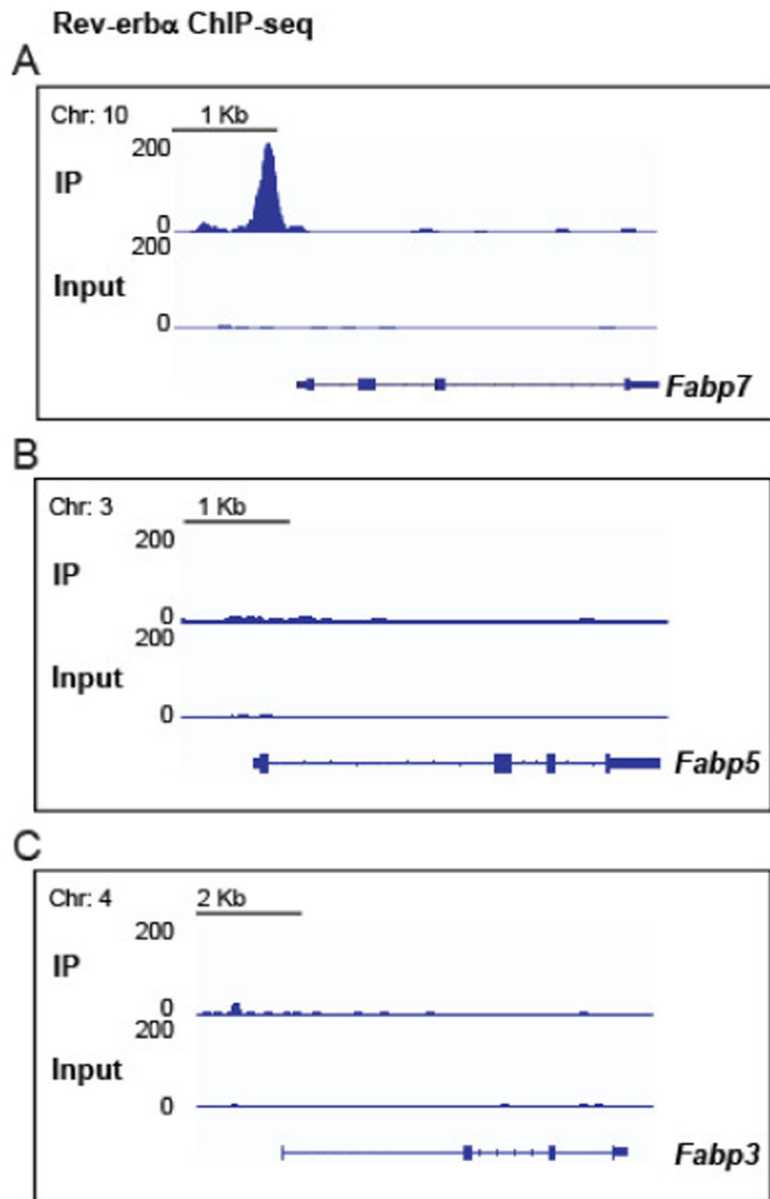


Figure 1. ChIP-seq binding profile of Rev-erb α around the *Fabp7* locus (A), but not in the *Fabp5* (B) or *Fabp3* (C) loci in the VTA of WT mice.

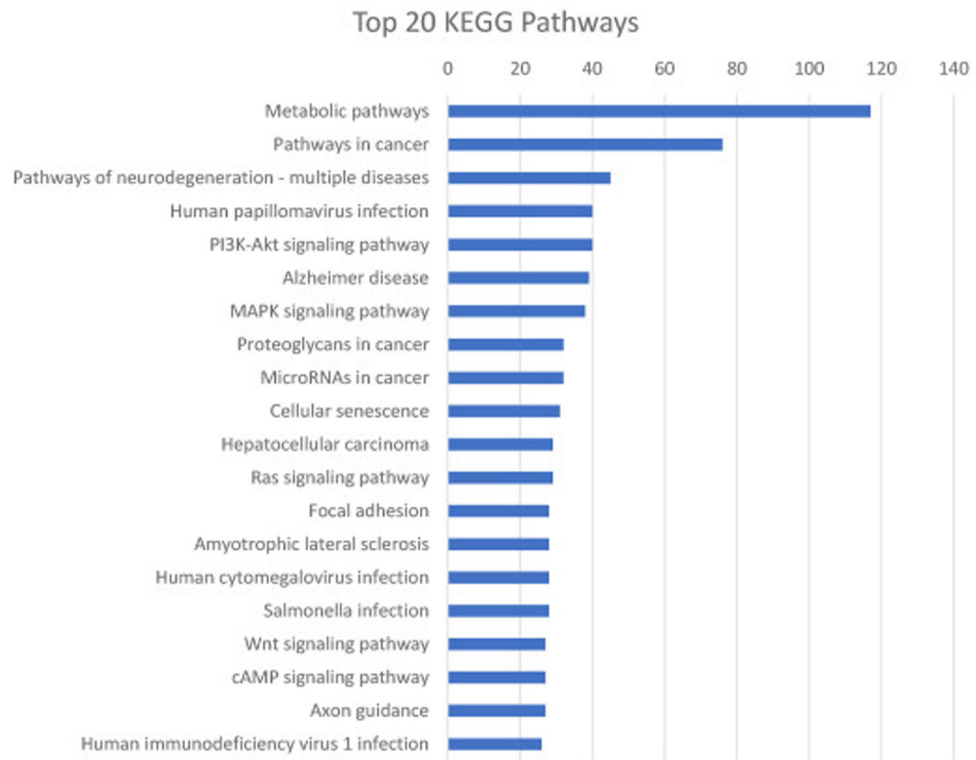


Figure 2. Analysis of the top 20 KEGG pathways enriched in Rev-erb ChIP-seq genes plotted with number of hits per pathway.

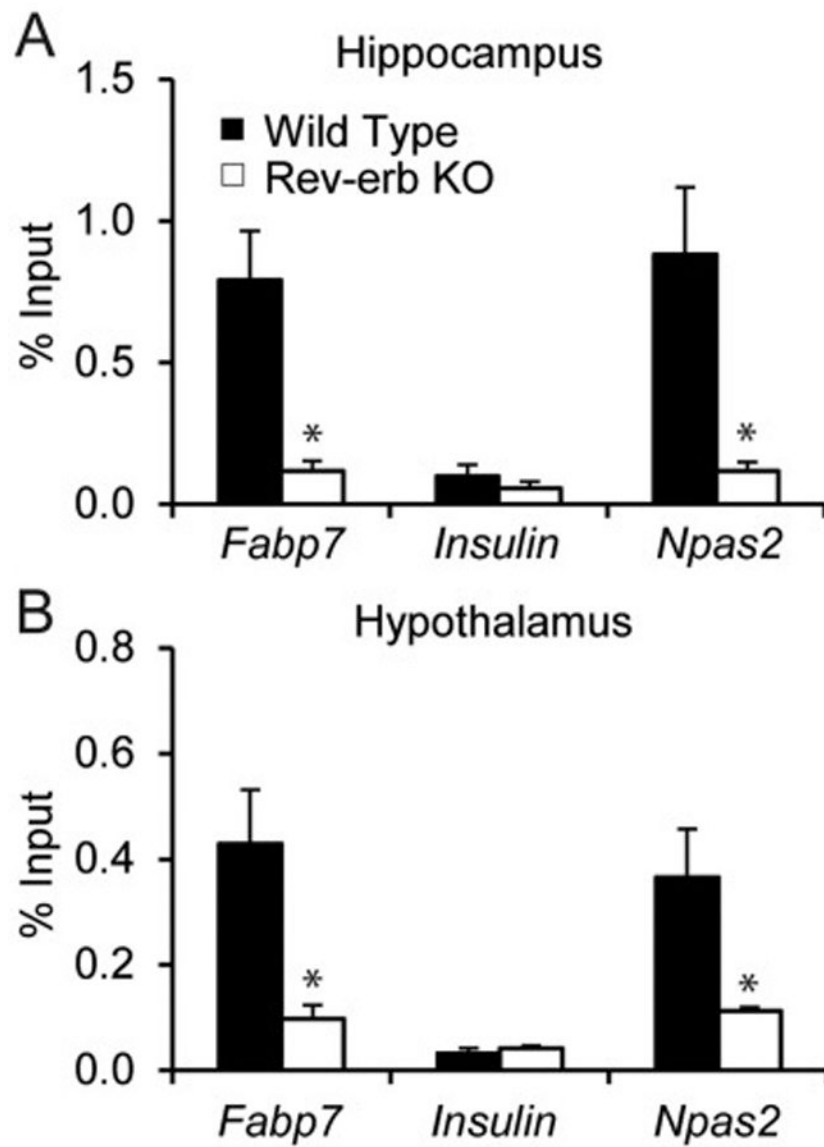


Figure 3. ChIP-qPCR measurements of Rev-erba relative occupancy at *Fabp7* locus, *Insulin* locus (negative control) and *Npas2* locus (positive control) in hippocampus (A) and hypothalamus (B) of WT and Rev-erba KO mice. Data are expressed as the percent of input and are the mean \pm SEM. (Student's t test, * $p < 0.05$, $n = 3$ per group).

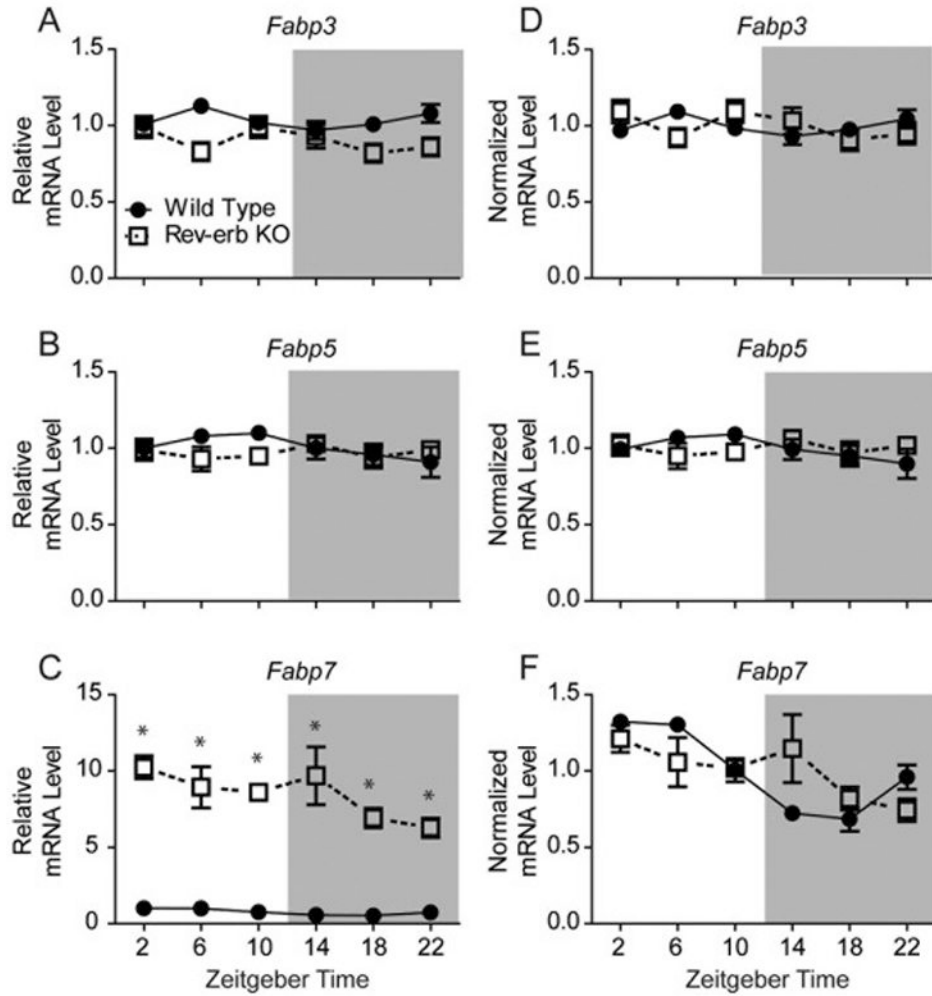


Figure 4.

A-C: Relative hippocampal mRNA expression of various Fabps in Rev-erba KO vs. WT mice under normal (LD) conditions. Levels of *Fabp3* (A) or *Fabp5* (B) are unaffected by Rev-erba deficiency, however, *Fabp7* shows a significant increase in expression based on genotype. * $p < 0.001$, $N = 4-7$ per group, Student's t-test. ZT=zeitgeber time. Hippocampal mRNA expression normalized to genotype to visualize the circadian rhythmicity of *Fabp3* (D), *Fabp5* (E), and *Fabp7* (F). *Fabp7* circadian rhythmicity was significantly disrupted in Rev-erba KO mice (adj. $p = 0.184$; JTK_Cycle) compared to WT mice (adj. $p < 0.001$; JTK_Cycle).

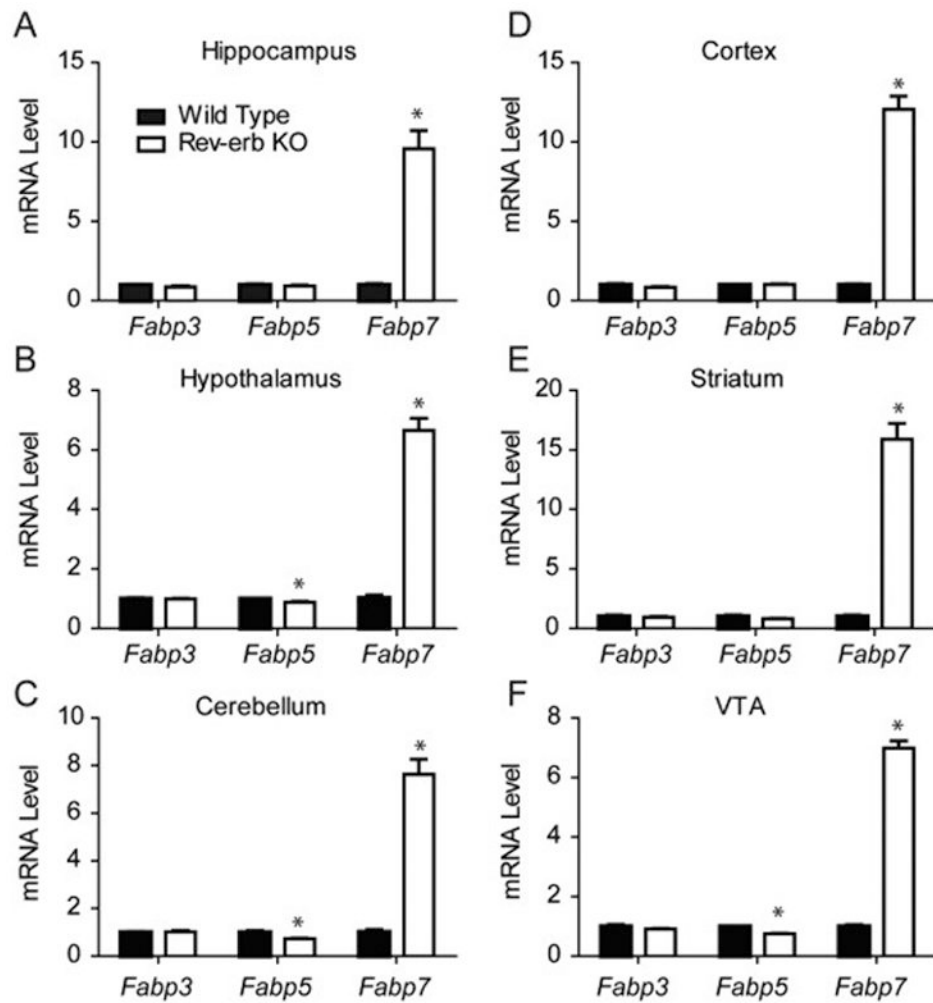


Figure 5.

A-F: Relative mRNA expression from various brain regions of *Fabps* in Rev-erba KO vs. WT mice. Levels of *Fabp3* mRNA are not affected by loss of Rev-erba, while lower levels of *Fabp5* mRNA are observed in Hypothalamus (B), Cerebellum (C), and VTA (F) based on Rev-erba deficiency compared to WT. *Fabp7* mRNA, however, shows significant increases in expression in Rev-erba KO compared to WT in all brain regions studied. * $p < 0.05$, ** $p < 0.01$, *** $p < 0.001$, $N = 3-5$ per group, Student's t-test.

Table 1.

The top 20 Rev-erba binding site loci, peak score, distance to the translational start site (TSS), and gene names, as identified by Rev-erba ChIP-seq.

Chromosome	Peak Score	Distance to TSS	Gene Name
chr14	151.18628	506	Nr1d2
chr1	139.22659	-2189	Igsf8
chr11	135.35667	-27206	Hlf
chr7	131.72737	2519	Dbp
chr7	102.16678	-206	Dbp
chr2	102.00463	10184	Cry2
chr11	97.30782	1526	Nr1d1
chr6	95.75218	9516	Bhlhe41
chr3	94.62258	-69	Ciart
chr6	81.56895	-1171	Bhlhe40
chr6	80.73732	83133	Lsm3
chr2	76.52149	401	Aven
chr11	76.4099	-4068	Per1
chr10	74.53577	-153	Fabp7
chr15	71.89268	-459	Tef
chr9	67.80914	-112	Nptn
chr1	62.37303	-197	Coq10b
chr16	61.30798	-793	Ubald1
chr7	60.32358	37	Arntl
chr15	59.34713	45290	Nfam1

Analysis of Gene Ontology in Rev-erba. ChIP-seq genes. Highest fold enriched Gene Ontology classes for Biological Process, Molecular Function and Cellular Component are listed with most highly enriched on top.

Table 2.

PANTHER GO-Slim Biological Process	Number of Genes	Fold Enrichment	Raw P-value	FDR
circadian regulation of gene expression	11	10.65	0.000000207	0.00000705
neg. reg. of transforming growth factor beta receptor signaling pathway	4	10.33	0.0021	0.0312
regulation of circadian rhythm	4	8.85	0.00314	0.0448
chondroitin sulfate proteoglycan biosynthetic process	5	6.46	0.00272	0.0393
protein demethylation	5	6.46	0.00272	0.0391
protein autophosphorylation	10	3.87	0.000719	0.0118
regulation of actin filament organization	15	2.8	0.000803	0.013
response to abiotic stimulus	16	2.75	0.000638	0.0106
positive regulation of transcription by RNA polymerase II	38	2.52	0.0000206	0.0000599
regulation of cellular component size	17	2.42	0.00196	0.0295
positive reg. of nucleobase-containing compound metabolic process	54	2.34	9.73E-08	0.00000342
PANTHER GO-Slim Molecular Function				
demethylase activity	9	5.17	0.000228	0.00452
flavin adenine dinucleotide binding	10	4.56	0.000242	0.00463
transcription coregulator activity	40	3.04	8.74E-09	0.00000606
phosphoprotein phosphatase activity	19	2.21	0.00295	0.0409
small molecule binding	44	1.76	0.000706	0.0112
protein kinase activity	51	1.62	0.00177	0.0266
PANTHER GO-Slim Cellular Component				
vacuolar membrane	13	2.76	0.00196	0.0344
Golgi membrane	14	2.55	0.00255	0.0418
transcription regulator complex	31	2.54	0.0000114	0.000386
neuron projection	42	1.72	0.00181	0.0328
transferase complex	50	1.69	0.000921	0.0187
bounding membrane of organelle	43	1.66	0.00248	0.0421
nucleoplasm	54	1.65	0.000836	0.0185
chromatin	67	1.56	0.000896	0.019